Selenomethionine mitigation of methylmercury-induced epigenetic and transcriptomic alterations in rainbow trout brain: a toxicogenomic survey

Marius Bidon, Takaya Saito, Kaja H Skjaerven, Philip Antony Jesu Prabhu, Cécile Heraud, Jérôme Roy, Claudia Marchán-Moreno, Zoyne Pedrero-Zayas, Stéphanie Fontagné-Dicharry

Aquatic Toxicology 291 (2026) 107706

Contents lists available at ScienceDirect

Aquatic Toxicology

journal homepage: www.elsevier.com/locate/aqtox

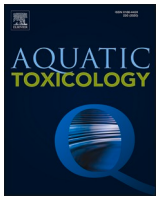

Selenomethionine mitigation of methylmercury-induced epigenetic and transcriptomic alterations in rainbow trout brain: A toxicogenomic survey

Marius Bidon [a,1], Takaya Saito [b,1], Kaja H. Skjaerven [b], Philip Antony Jesu Prabhu [b,2], Cécile Heraud [a], Jérôme Roy [a], Claudia Marchán-Moreno [c], Zoyne Pedrero-Zayas [c], Stéphanie Fontagné-Dicharry [a,*]

[a] INRAE, University of Pau and Pays de l'Adour, E2S UPPA, NUMEA, 64310 Saint-Pee-sur-Nivelle, France
[b] Feed and Nutrition group, Institute of Marine Research, Bergen 5817, Norway
[c] Université de Pau et des Pays de l'Adour, E2S UPPA, CNRS, IPREM, Institut des Sciences Analytiques et de Physico-chimie pour l'Environnement et les matériaux, Pau, France

ARTICLE INFO

Keywords:
Methylmercury
Selenomethionine
Toxicogenomics
Brain
Rainbow trout

ABSTRACT

Methylmercury (MeHg) is a pervasive neurotoxicant threatening aquatic ecosystems. Selenium (Se) has been reported to protect fish against the adverse MeHg toxicity, yet molecular investigations of their interaction in the brain remain scarce. This study investigated the molecular effects of dietary MeHg and whether organic Se, in the form of selenomethionine (SeMet), could mitigate MeHg-induced change in the brain of rainbow trout (*Oncorhynchus mykiss*). A 6-month feeding trial was conducted with diets containing low basal Se (0.3 mg/kg) and no mercury (Hg), supplemented with 2 mg Hg/kg diet as MeHg, alone or combined with 1.5 mg Se/kg diet as SeMet. Gene methylation (reduced representation bisulfite sequencing) and expression (RNA sequencing) were assessed, alongside biochemical quantification of DNA methylation-related metabolites (S-adenosylmethionine, SAM, and S-adenosylhomocysteine, SAH) and oxidative stress-related metabolites (reduced glutathione, GSH, and oxidized glutathione, GSSG). SeMet did not prevent MeHg-induced changes in SAM/SAH levels but mitigated MeHg-induced alterations in DNA methylation of genes related to the glutamatergic system, inflammation, and immune response. Transcriptomic analysis revealed antagonistic effects of MeHg and SeMet on energy metabolism pathways, with *hypoxia-inducible factor 1 subunit alpha-like 2* identified as a potential key regulator. Although this molecular interaction may reflect SeMet-mediated attenuation of oxidative stress, biochemical data did not confirm changes in GSH/GSSG levels. These findings provide novel insights into the molecular mechanisms underlying MeHg neurotoxicity and its modulation by SeMet in fish brain, highlighting a potential protective role of organic Se against MeHg-induced molecular alterations.

1. Introduction

Mercury (Hg) is a pervasive environmental contaminant that poses a significant threat to wildlife and ecosystems, particularly aquatic ones (Okeke et al., 2024). Since the beginning of the anthropogenic era, surface ocean Hg concentrations have increased threefold (Lamborg et al., 2014). Approximately 80 % of Hg is deposited in the ocean in inorganic form (Horowitz et al., 2017), which is then converted by microorganisms into methylmercury (MeHg) (Hsu-Kim et al., 2013). This organic form of Hg is considered a major concern for the aquatic environment (Jeong et al., 2024) due to its ability to biomagnify through the food chain (Nfon et al., 2009; Scheuhammer et al., 2015). Consequently, MeHg is the predominant form of Hg found in fish (Cressey et al., 2020), where the dietary intake is the main route of exposure and accumulation (Hall et al., 1997). Piscivorous species at higher trophic levels typically bioaccumulate greater MeHg levels (Lavoie et al., 2013), increasing their vulnerability to MeHg toxicity (Wiener et al., 2002).

The nervous system is the primary target of MeHg toxicity (Fernandes Azevedo et al., 2012). In fish, dietary MeHg exposure has been associated with brain lesion (Berntssen et al., 2003),

* Corresponding author.
E-mail address: stephanie.fontagne-dicharry@inrae.fr (S. Fontagné-Dicharry).
[1] These authors contributed equally to this work.
[2] Present address: Nutrition and Feed technology group, Nofima, Bergen 5141, Norway.

https://doi.org/10.1016/j.aquatox.2026.107706
Received 19 October 2025; Received in revised form 30 December 2025; Accepted 2 January 2026
Available online 3 January 2026

neurobehavioral impairments, and neurochemical alterations (Nielsen et al., 2016). Mechanistically, MeHg can induce oxidative stress (Berntssen et al., 2003; Cardoso et al., 2017), disrupt energy metabolism, impair mitochondrial function, alter calcium homeostasis, and interfere with microtubule organization (Berg et al., 2010; Rasinger et al., 2017). Genome-wide approaches have substantially improved the understanding of the molecular mechanisms of MeHg in fish exposed through diet (Klaper et al., 2006; Liu et al., 2013). However, such approaches have not yet been applied to the brains of fish exposed to dietary MeHg. Moreover, DNA methylation, a key epigenetic mechanism involved in gene regulation (McCarrey, 2003; Moore et al., 2013), has been proposed to mediate MeHg effects (Culbreth and Aschner, 2019). Yellow perch (*Perca flavescens*) exposed to MeHg-contaminated diet showed no changes in global brain DNA methylation (Basu et al., 2013). Yet, more sensitive methylomic analyses could reveal subtle alterations in DNA methylation, relevant to MeHg neurotoxicity mechanisms.

Selenium (Se), an essential trace element, is known to reduce MeHg accumulation in fish when present in food (Bjerregaard et al., 2011) and to protect the fish brain against adverse MeHg effects, mainly by mitigating oxidative stress (Baldissera et al., 2020). Therefore, the Se:Hg molar ratio in the diet has been proposed as a toxicological parameter to assess and predict the potential adverse effects of dietary Hg exposure (Ralston et al., 2016). More recently, it was demonstrated that the Se:Hg molar ratio should be considered alongside selenium speciation in the diet to improve Hg risk assessment (Fernández-Bautista et al., 2024). Indeed, Se can exist in various forms, and our previous study on the same set of fish revealed that Se bioaccumulates at higher concentrations in the brains of rainbow trout (*Oncorhynchus mykiss*) when supplied as selenomethionine (SeMet), an organic form rather than as sodium selenite, an inorganic form (Marchán-Moreno et al., 2024). Thus, given its higher bioaccumulation, SeMet might provide stronger protection against MeHg toxicity, but mechanistic evidence in fish remains scarce. A proteomic survey in the brains of zebrafish (*Danio rerio*) exposed to dietary MeHg and SeMet showed that the mammalian target of rapamycin pathway was activated by MeHg, but inhibited when SeMet was added concomitantly (Rasinger et al., 2017). Transcriptomic studies on dietary MeHg/SeMet interactions exist only in the mammalian brain, where effects on gene expression related to oxidative stress and inflammation have been observed (Mellingen et al., 2022). Furthermore, a study in rainbow trout livers showed that dietary hydroxy-SeMet may influence DNA methylation by altering the levels of S-adenosylmethionine (SAM) and S-adenosylhomocysteine (SAH), two key metabolites in methylation processes (Wischhusen et al., 2020). The same study also reported that this dietary organic Se form affected the methylation status of genes involved in neurotransmission and immunity. These findings suggest that methylomic approaches represent a promising way to study the interactions between dietary SeMet and MeHg in the fish brain, offering new insights into how SeMet may protect against MeHg toxicity.

Here we investigated the molecular effects of chronic dietary exposure to MeHg, alone or in combination with SeMet, in the brains of juvenile rainbow trout, a piscivorous species. Fish were exposed for six months to environmentally relevant levels of MeHg (2 ppm). The MeHg concentration of 2 ppm refers to dry weight in fish meal or fish tissue. This corresponds to approximately 0.4–0.5 ppm on a wet weight basis, which falls within the range reported for predatory fish (Scheuhammer et al., 2015; Mille et al., 2021; Barbosa et al., 2022). Hg concentrations in wild fish associated with symptoms of MeHg toxicity typically range from 0.3 to 0.7 ppm in the whole body and from 0.5 to 1.2 ppm in muscle (Sandheinrich and Wiener, 2011). In top marine predators such as tunas, levels can reach 1.2 ppm in muscle or 1.8 ppm in blood (Barbosa et al., 2022). Diets were also supplemented with 1.5 ppm of SeMet, concomitantly with MeHg. This SeMet supplementation remains below the established safe feed limit of 2.8 ppm in salmon (*Salmo salar*), above which adverse effects begin to be observed (Berntssen et al., 2018). This supplementation also allowed us to achieve a dietary Se:Hg molar ratio above 1, which has been shown to counteract the adverse effects of Hg in fish (Peterson et al., 2009). To elucidate the neurotoxic effects of MeHg and the potential protective role of SeMet, we employed an integrative multi-omics approach combining methylomics (reduced representation bisulfite sequencing, RRBS) and transcriptomics (RNA sequencing, RNA-seq). RRBS is a targeted DNA methylation profiling method that enriches for CpG-dense and regulatory regions of the genome, allowing quantitative assessment of cytosine methylation at single-base resolution. In this study, RRBS was applied to investigate whether chronic MeHg and/or SeMet exposure induces epigenetic modifications that might explain further the protection of SeMet against MeHg influences, that remain to date under-investigated. In parallel, we measured SAM and SAH levels as potential indicators of DNA methylation status (Caudill et al., 2001), and assessed reduced (GSH) and oxidized (GSSG) forms of glutathione, commonly used as markers of oxidative stress (Sies et al., 2017) in trout brains.

By combining these complementary approaches, our study aims to advance understanding of the molecular mechanisms underlying MeHg neurotoxicity and dietary SeMet-mediated protection in fish, addressing critical gaps in current knowledge.

2. Material and methods

2.1. Experimental fish and dietary trial conditions

The experimental design, rearing conditions, and diet preparation were previously described in detail (Bidon et al., 2023). All experimental procedures were conducted in accordance with European Union Directive 2010/63/EU and French Decree no 2013–118 on animal experimentation, with ethical approval from the C2EA-73 committee and authorization from the French Ministry of Higher Education and Research (project agreement number: APAFIS#27,846–2020102812241350v2). Briefly, all-female diploid rainbow trout juveniles (initial body weight: 26 ± 1 g) were reared for six months at the INRAE experimental facilities in Donzacq, France (https://doi.org/10.15454/GPYD-AM38). Fish were hand-fed twice daily to visual satiation with practical diets formulated with plant-derived proteins (Table 1). These diets were isonitrogenous (49% crude protein), isolipidic (22% total lipid), and isocaloric (25 kJ/g) differing only in Se and Hg content. The control negative diet (PC) contained baseline levels of 0.3 mg Se/kg and < 0.01 mg Hg/kg, without any additional supplementation. The MeHg diet (PH) was supplemented with 2 mg Hg/kg, provided as methylmercury(II) chloride (Sigma-Aldrich, France), resulting in dietary concentrations of 0.3 mg Se/kg and 2.6 mg Hg/kg. The MeHg and SeMet diet (PHO) combined the same MeHg supplementation (2 mg Hg/kg) with an additional 1.5 mg Se/kg as L-selenomethionine (Excential Selenium 4000, Orffa, Netherlands), achieving dietary levels of 2.2 mg Se/kg and 2.4 mg Hg/kg.

After 168 days of feeding, fish were starved overnight (16 h) before sampling. Eight fish per tank were randomly selected, anaesthetized using benzocaine at a concentration of 30 mg/L, and then euthanized with a benzocaine solution at 60 mg/L. Final body weights of fish were measured, with no significant differences observed between treatments. Mean final body weights were 400 ± 13 g (control diet PC), 420 ± 19 g (MeHg diet PH), and 424 ± 11 g (MeHg and SeMet diet PHO), based on three replicate tanks per group.

Whole fish brains were collected, snap-frozen in liquid nitrogen, and stored at −80 °C for subsequent analysis. Total Hg and Se concentrations in brain tissues were measured in three individual fish per dietary treatment (one fish per tank), as detailed elsewhere (Marchán-Moreno et al., 2024). In brief, Hg was undetectable in the brains of control fish (PC), while exposure to MeHg (PH) and MeHg and SeMet (PHO) resulted in Hg concentrations of 2.36 ± 0.40 μg/g and 1.94 ± 0.23 μg/g wet weight, respectively, with no significant reduction due to Se addition. Similarly, Se concentrations in the brain were 0.62 ± 0.05 μg/g (PC), 1.08 ± 0.02 μg/g (PH), and 26.8 ± 2.2 μg/g (PHO). Dietary MeHg did not significantly affect brain Se levels.

Table 1
Experimental plant-based diet formulation, composition, levels of supplementations for L-selenomethionine and methylmercury(II) chloride and elemental composition of plant-based diets: control plant-based diet (PC), plant-based diet supplemented with methylmercury(II) chloride (PH), plant-based diet supplemented with methylmercury(II) chloride and L-selenomethionine (PHO).

Plant-based diet	PC	PH	PHO
Ingredients (%)			
Plant-derived proteins[a]	73.8	73.8	73.8
Crystalline amino acid premix[b]	3.2	3.2	3.2
Rapeseed lecithin[c]	2	2	2
Vegetable oils[d]	8	8	8
Fish oil[e]	8	8	8
Vitamin and mineral premixes[f]	5	5	5
Levels of supplementation (mg/kg diet)			
Selenium as Excential selenium 4000[g]	-	-	1.5
Mercury as methylmercuryII chloride[h]	-	2	2
Elemental composition (mg/kg ww diet, n = 3)			
Selenium (Se)	0.25 ± 0.02	0.28 ± 0.01	2.20 ± 0.01
Mercury (Hg)	-	2.6 ± 0.2	2.4 ± 0.2
Se:Hg molar ratio	-	0.4	2.6

[a] Plant-derived proteins (% diet): wheat gluten, 18 (Roquette, France); corn gluten, 17 (Inzo, France); soybean protein concentrate, 15 (Estril®75 Sopropêche, France); soybean meal, 5 (Sud-Ouest Aliment, France); white lupin meal, 5 (Farilup500 Terrena, France); rapeseed meal, 5 (Primor 00 Sud-Ouest Aliment, France), dehulled pea mea, 3.8 (Primatex Sotexpro, France), whole wheat, 5 (Sud-Ouest Aliment, France).

[b] Crystalline amino acid premix (% diet): L-lysine, 1.4; DL-methionine, 0.3; glucosamine, 0.5; taurine, 0.3; betaine, 0.3; glycine, 0.2; alanine, 0.2.

[c] Adivec (Orléans, France).

[d] Vegetable oils (% diet): rapeseed oil, 4; linseed oil, 2.4; palm oil 1.6.

[e] Sopropêche (Wimille, France).

[f] Vitamin and mineral premixes Se-free (per kg diet): retinyl acetate, 5000 IU; cholecalciferol, 2500 IU; DL-α-tocopheryl acetate, 50 IU; sodium menadione bisulfate, 10 mg, thiamin-HCl, 1 mg; riboflavin, 4 mg; niacin, 10 mg; D-calcium pantothenate, 20 mg; pyridoxine-HCl, 3 mg; myo-inositol, 0.3 g; D-biotin, 0.2 mg; folic acid, 1 mg; cyanocobalamin, 0.01 mg; L-ascorbyl-2-polyphosphate, 50 mg; choline-HCl, 1 g; $CaHPO_4.2H_2O$ (18% P; 22% Ca), 33g; $CaCO_3$ (40% Ca),·2.15 g; $MgOH_2$ (42% Mg), 1.24 g; KCl (52% K), 0.9 g; NaCl (39% Na), 0.4 g; $FeSO_4·H_2O$ (33% Fe), 20 mg; $ZnSO_4·H_2O$ (36% Zn), 35 mg; MnO (77%); 10 mg; $CuSO_4·5H_2O$ (25% Cu), 5 mg; NaF (45% F), 10 mg; CaI_2 (86% I), 3 mg; $CoCO_3$ (50% Co), 0.05 mg; BHA, 0.75 mg; BHT, 0.75 mg; propyl gallate, 0.15 mg; sepiolite, 200 mg. All ingredients were diluted with α-cellulose.

[g] Orffa (Breda, The Netherlands), contains 0.4% L-selenomethionine.

[h] Sigma-Aldrich (Saint-Quentin-Fallavier, France).

2.2. Determination of brain GSH and SAM metabolites

The levels of SAM, SAH, GSH, and GSSG in frozen brain tissues (n = 2 individual brains per tank, i.e. n = 6 per dietary treatment) were quantified using high-performance liquid chromatography coupled with ultraviolet detection.

Brain samples were weighed and homogenized with zirconium beads in a Precellys® 24 homogenizer (Bertin Technologies, France) for two 10-s cycles at a milling speed of 5500 rotations per min, using 100 µL of phosphate buffer (20 mM, 1 mM EDTA, pH 6.5 ± 0.05). The homogenate was centrifuged at 14,000 × g for 20 min at 4°C and deproteinized by mixing with 280 µL of 10 % (w/v) metaphosphoric acid in a 1/1 ratio. After thorough mixing and a subsequent centrifugation at 14,000 × g for 5 min at 4°C, the supernatant was filtered through a 0.22 µm polyvinylidene fluoride filter and stored at -20°C until analysis.

Chromatographic separation was achieved on a Symmetry Shield RP18 column (150 × 4.6 mm, 3.5 µm, 100Å; Waters, MA, USA) maintained at 30°C. Injection volumes were 50 µL for standards and 100 µL for samples. Standards for GSH, GSSG, SAM, and SAH (Sigma-Aldrich) were prepared in 5 mM HCl to generate external calibration curves ranging from 500 to 5 µM for GSH, 20 to 0.5 µM for GSSG, and 5 to 0.125 µM for SAM and SAH. The mobile phase consisted of 20 mM phosphate buffer at pH 2.7 (solvent A), acetonitrile (solvent B), ultrapure water (solvent C), and methanol (solvent D), with the following gradient: 0-10 min, 99.5 % A and 0.5 % D; 12-15 min, 40 % A and 60 % B; 17-30 min, 99.5 % A and 0.5 % D. Detection was performed simultaneously at 210 nm for GSH and GSSG, and at 258 nm for SAM and SAH, based on their respective retention times.

Total protein content in brain samples was determined using a bicinchoninic acid assay. Briefly, 5 µL of homogenized brain sample, diluted 1/25 in ultrapure water, was mixed with 200 µL of working reagent (50 parts bicinchoninic acid reagent to 1 part copper sulfate) (#BCA1-1KT, Sigma-Aldrich). After incubation at 37°C for 30 min, absorbance was measured at 562 nm. Protein concentrations were calculated using an external standard curve with bovine serum albumin.

2.3. DNA and RNA extraction

For DNA and RNA extraction, the same fish brains were used, with six individual brains analyzed per dietary treatment (n = 2 per tank) and allow to obtain relative expression data and DNA methylation levels in the same individual. Methods for DNA and RNA extraction have been described previously (Saito et al., 2021). Brain tissues were homogenized using ceramic beads CK28 in a Precellys® 24 homogenizer. A portion of the homogenate was allocated for RNA extraction using the BioRobot EZ1 and EZ1 RNA Universal Tissue Kit (Qiagen, Germany). To prevent DNA contamination, homogenates underwent DNase treatment with the Ambion DNA-free DNA removal kit (Invitrogen, USA), following the manufacturer's instructions. RNA quantity and purity (A260/280 and A260/230 ratios) were assessed for each sample using a NanoDrop ND-1000 Spectrophotometer.

The remaining portion of the homogenate was treated with RNase A (provided by the Qiagen kit, 50 ng/µL, 10 min at room temperature) and proteinase K (New England Biolabs, #8102S 20 µg/µL, 1.5 h at 55°C) prior to DNA extraction using the DNeasy Blood & Tissue Kit (Qiagen, Germany), following the manufacturer's protocol. DNA was eluted in Milli Q water. Quantification of double-stranded genomic DNA was performed using the Qubit High Sensitivity Assay (Life Technologies, CA, USA).

2.4. Reduced representation bisulfite sequencing (RRBS) library preparation and sequencing

RRBS library preparation can be found in details elsewhere (Saito et al., 2021). Up to 100 ng of DNA extracts were used for RRBS library preparation. DNA extracts were digested with the MspI enzyme (20 U, New England BioLabs, UK) for 12 h at 37°C in 30 µL reaction containing 1X NEB buffer. The digested DNA fragments were subsequently end-repaired and A-tailed by adding the Klenow fragment 3'->5' exo (Enzymatics, MA, USA) and a dNTP mix (10 mM dATP, 1 mM dCTP, 1 mM dGTP, New England BioLabs).

Adaptors ligation was performed using methylated Illumina TruSeq LT v2 adaptors and DNA Ligase Rapid (Enzymatics, MA, USA). A size selection of the library was then carried out using a 0.75 X clean-up with AMPure XP beads (Beckman Coulter, CA, USA). Following size selection, the DNA library was bisulfite-converted using the EZ DNA Methylation Direct Kit (Zymo Research, CA, USA), following the manufacturer's protocol with these modifications: the conversion reagent was used at a 0.9 X concentration, the incubation involved 20 cycles of 1 min at 95°C and 10 min at 60°C, and the desulphonation step lasted 30 min.

This bisulfite-converted library was enriched using KAPA HiFi HS Uracil$^+$ RM (Roche, Switzerland). Library clean-up was performed with 1 X AMPure XP bead clean-up and library quantification was carried out using the Qubit Fluorometric Quantification System (Life Technologies, CA, USA). The size distribution of the library was assessed using a Bioanalyzer High Sensitivity DNA Kit (Agilent, CA, USA).

Finally, RRBS libraries were sequenced on the Illumina HiSeq 4000 platform in 50-base-pair single-end mode at the Research Center for

Molecular Medicine of the Austrian Academy of Sciences (CeMM) Biomedical Sequencing Facility (Vienna, Austria). Sequencing data from each sample were processed and converted into single Binary Alignment/Map (BAM) files. The files, along with sample descriptions and RRBS library preparation methods, were uploaded to the Sequence Read Archive/BioProject repository at the National Center for Biotechnology Information (NCBI; BioProject accession number: PRJNA803611).

2.5. RNA-seq library preparation and sequencing

RNA-seq library preparation can be found in details elsewhere (Saito et al., 2021). The cDNA library for transcriptome sequencing was prepared using the NEBNext Ultra RNA Library Prep Kit (New England BioLabs), following the manufacturer's instructions. Sequencing was performed on the Illumina NovaSeq 6000 platform at the Novogene UK Sequencing Centre (Cambridge, UK).

The sequencing output consisted of FASTQ files, with two files per sample corresponding to paired-end reads. The sequencing files, along with sample descriptions and details of the RNA-seq library preparation method, were deposited in the SRA/BioProject repository at NCBI (BioProject accession number: PRJNA781457).

2.6. Rainbow trout genome and genomic annotation

The rainbow trout genome (OmykA_1.0, annotation release 100) used for the analysis was downloaded from the NCBI assembly site (https://www.ncbi.nlm.nih.gov/assembly/ GCF_002163495.1). The genome was divided into several genomic regions as follows: gene body, promoter, flanking regions (flank) and intergenic regions. The gene body was further subdivided into exons and introns. The promoter region was categorized based on the distance from the transcription start site (TSS) as follows: proximal promoter (P250, 1 bp to 250 bp from the TSS), promoter region (P1K, 251 bp to 1000 bp from the TSS), and distal promoter (P5K, 1001 bp to 5000 bp from the TSS). Flanking regions were classified as "flank up" (5K, upstream from the 5′ end of P5K) and "flank down" (10K, downstream of the 3′ end of the mRNA). Finally, intergenic regions were defined as areas outside of the gene bodies, promoters, and flanking regions.

2.7. RRBS workflow analysis

First, the quality of the RRBS sequencing was assessed for the 18 BAM files using FastQC (Babraham Institute; https://www.babraham.ac.uk) and MultiQC (Ewels et al., 2016). The 18 BAM files were then converted into FASTQ files for processing with TrimGalore! (Babraham Institute). The RRBS mode of TrimGalore! was used to check for potential adapter contaminants and low-quality reads (Phred scores less than 20 and reads shorter than 20 nucleotides) and to remove them. The trimming process was evaluated using MultiQC report.

Trimmed reads were aligned to the reference genome (OmykA_1.0, annotation release 100, FASTA format) using Bismark with default parameters (Krueger and Andrews, 2011). The reference genome was first indexed by Bismark. The alignment process generated BAM files for each sample. The alignment results were reviewed using MultiQC to determine the percentage of reads that aligned or were ambiguously aligned.

Next, methylation rates of cytosines in CpG, CHG and CHH contexts (where H represents any nucleotide other than C) were extracted using the bismark_methylation_extractor function provided by Bismark. A MultiQC report was generated to check the extraction process. Cytosines in the CpG context were then further extracted using the methRead function from the methylKit package. During this extraction step, cytosines in the CpG sites were filtered using the filterByCoverage function from methylKit (Akalin et al., 2012). Cytosines with fewer than 10 counts or those above the 99.9th percentile of coverage were discarded.

Samples were then grouped based on the dietary treatment using unite function from the methylKit package, and the following comparisons were performed: PH:PC, PHO:PC (with PC as the control), and PHO:PH (with PH as the control). CpG-united sites were counted, and the methylation rates were visualized through principal component analysis (PCA), hierarchical clustering, and heat maps.

Differentially methylated cytosines (DMCs) in the CpG context were identified using calculateDiffMeth function from the methylKit package for the comparisons described above. The input for the calculateDiffMeth function consisted of the methylation rates of united CpG sites, generated by the union function in methylKit. A p-value was calculated using logistic regression, and a q-value (adjusted p-value) was calculated using the sliding linear model method (Wang et al., 2011). A cytosine in the CpG context was considered differentially methylated when the q-value was less than 0.01 and the methylation difference was greater than 20 %. A negative percentage of methylation indicated hypo-methylation, while a positive percentage indicated hyper-methylation.

The list of DMCs was associated with genomic regions of the OmykA_1.0 genome. The reference genome was first converted into a GRanges object using the GenomicRanges library (Lawrence et al., 2013). DMCs were then assigned to the previously defined genomic regions. DMCs were counted and summarized by genomic region. Genes with at least one DMC in their gene body or regulatory sequences (promoter and flanking regions) were considered differentially methylated genes (DMGs).

2.8. RNA-seq workflow analysis

Quality control was performed on the 36 FASTQ files (from 18 samples) using MultiQC (Ewels et al., 2016). This report provided an overview of sequencing quality and highlighted potential issues, such as poor sequencing depth or overrepresented sequences caused by polymerase chain reaction artifacts or adapter contamination. To address these concerns, adapter contamination and low-quality reads (Phred scores below 20 and reads shorter than 20 nucleotides) were identified and removed from the FASTQ files using TrimGalore! with the Cutadapt function. The results of this trimming process were summarized in a MultiQC report.

The trimmed reads were then aligned to the reference genome of rainbow trout (OmykA_1.0, annotation release 100) using the STAR aligner software (Dobin et al., 2013). Paired-end reads for each sample were aligned, and a single output file (BAM format) was generated per sample (18 files in total). The quality of the alignment, including metrics such as the number of aligned, unmapped and uniquely mapped reads, was assessed with a MultiQC report.

Aligned reads were quantified per gene using the featureCounts function from the Subread package (Liao et al., 2014). An index of the annotated rainbow trout genome was first created, and reads were counted for each gene based on overlap with at least one exon. Summary reports were generated with MultiQC to evaluate how many transcripts were successfully assigned to the reference genome.

To prepare the data for PCA, raw counts were transformed using the variance-stabilizing transformation (vst) function from the DESeq2 package (Love et al., 2014). PCA was performed to visualize sample clustering and detect potential outliers.

Differential expression (DE) analysis was conducted using DESeq2 on raw count data. The Wald test was used to calculate p-values, while the Benjamini-Hochberg method was applied to adjust p-values for multiple testing. Genes were considered differentially expressed (DEGs) if their adjusted p-value $\leq$ 0.1, the default significance threshold used in DESeq2.

To assess biological pathways, gene set enrichment analysis (GSEA) was performed for all genes mapped to the reference genome using the

Kyoto Encyclopedia of Genes and Genomes (KEGG) database for rainbow trout (Kanehisa and Goto, 2000) and Gene Ontology (GO) databases. The analysis was conducted using the R package clusterProfiler (Yu et al., 2012). Pathways were considered significantly enriched if the hypergeometric test returned an adjusted p-value ≤ 0.05.

Finally, density-based clustering was performed using the Density-Based Spatial Clustering of Applications with Noise (DBSCAN) algorithm (Ester et al., 1996) via the R package dbscan (Hahsler et al., 2019). Input data consisted of differences in mean normalized read counts (PH - PC, PHO - PC, and PHO - PH) calculated using the trimmed mean of M-values (TMM) normalization method from edgeR (Robinson et al., 2010). The parameters for DBSCAN were set to 27 for the minimum number of points (minPts) and 3.3 for the epsilon neighborhood size (eps).

2.9. Statistical analysis

All statistical analyses were performed using R software (version 3.6.1, R Core Team, 2019). Statistical significance was set at p-value ≤ 0.05. GSH/GSSG, and SAM/SAH levels in the brain were expressed as mean ± standard error of the mean (SEM). To assess differences among dietary treatments, a one-way analysis of variance (ANOVA) was conducted.

The assumptions required for the validity of the one-way ANOVA, namely normality and homoscedasticity, were verified using the Shapiro-Wilk test and Levene's test, respectively. When the ANOVA returned significant results (p-value ≤ 0.05), a Tukey's post-hoc test was performed to evaluate pairwise comparisons between dietary treatments.

In cases where the assumptions for ANOVA were not met, a non-parametric Kruskal-Wallis test was applied. If the Kruskal-Wallis test indicated significant differences, pairwise comparisons were conducted using Dunn's post-hoc test.

3. Results

3.1. Effects of dietary MeHg exposure, alone or combined with SeMet, on brain metabolites of methylation potential and oxidative stress

Fish exposed to dietary MeHg, either alone or in combination with SeMet, exhibited lower SAH levels (0.28-fold and 0.25-fold reductions, respectively) (Fig. 1A) and decreased GSSG levels (0.42-fold and 0.32-fold reductions, respectively) (Fig. 1B) compared to the control group. However, both exposure groups showed an increased SAM/SAH ratio (0.34-fold and 0.21-fold increases, respectively) (Fig. 1A) and higher GSH/GSSG ratio (0.50-fold and 0.35-fold increases, respectively) (Fig. 1B) relative to the control. While SAM levels in the brain remained unaffected by dietary MeHg exposure, fish co-exposed to MeHg and SeMet displayed a significant reduction in SAM levels (0.13-fold) compared to the control (Fig. 1A).

3.2. Effects of dietary MeHg exposure, alone or combined with SeMet, on the brain methylome

Details of the alignment step in the RRBS analysis are provided in **Supplementary Table S1**.

In the PH:PC pairwise comparison, a total of 7,202 DMCs were identified, 4,473 of which had a unique localization (chromosome number + position on the chromosome, (Fig. 2A). In the PHO:PC comparison, 7,460 DMCs were detected, including 4,485 that were unique to this condition. The highest number of DMCs was observed in the PHO:PH comparison, with 12,252 DMCs, of which 10,429 were exclusive to this comparison. Across conditions, 1,901 DMCs were shared between PH:PC and PHO:PC, while 995 DMCs were common between PHO:PC and PHO:PH. Additionally, 749 DMCs were found in both the PH:PC and PHO:PH comparisons. Notably, 79 DMCs were consistently identified at the same positions in all three pairwise comparisons.

Despite variations in the total number of DMCs across comparisons, a balanced distribution between hypo- and hypermethylated DMCs was

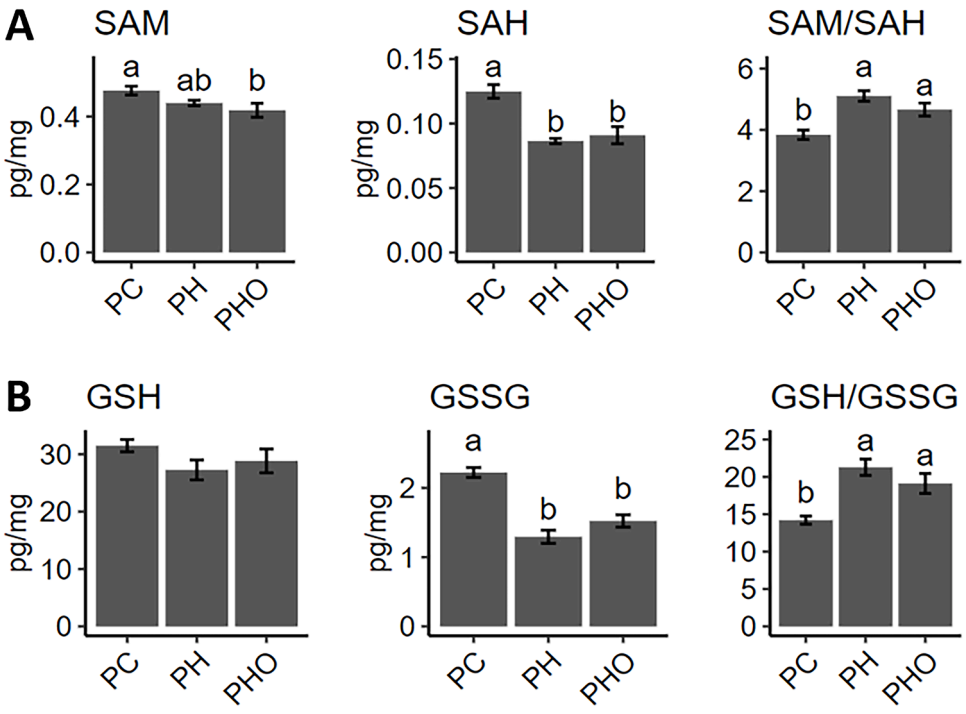

Fig. 1. A: SAM/SAH concentrations (pg/mg of proteins) and SAM/SAH ratio (n = 6); B: GSH/GSSG concentrations (pg/mg of proteins) and GSH/GSSG ratio (n = 6) in brain of rainbow trout fed with a control diet (PC), supplemented with MeHg solely (PH) or a combination with SeMet (PHO) for six months. Bars represent the mean ± standard error mean. For the analysis a one-way ANOVA was performed followed by a Tukey post hoc test. Means with a different superscript letter underline a significant difference (p-value ≤ 0.05), according to the one-way ANOVA followed by Tukey post hoc test.

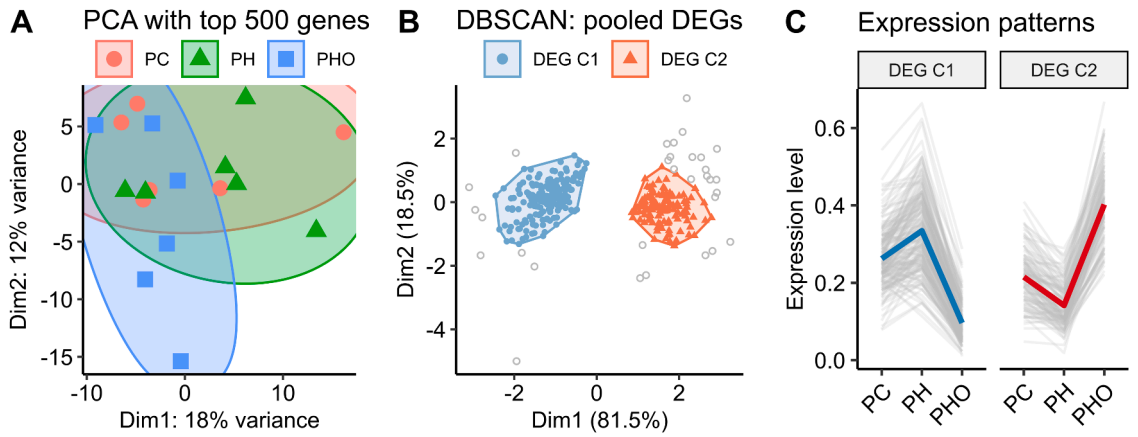

Fig. 2. A: Venn diagram of methylated cytosine position (chromosome number + position on chromosome) for the three pairwise comparison PH:PC, PHO:PC and PHO:PH; B: Total number of DMCs hypo or hyper-methylated in the three pairwise comparisons; C: Violon plots with DMCs (methylation percentage ≥ or ≤ 20 %) counts of hypo or hypermethylated cytosines depending on gene region: exon, intron, promotor (P250, P1K and P5K), flank, intergenic region (IGR).

observed in all cases DMCs (Fig. 2B and **Supplementary Table S2**). In the PH:PC comparison, 3,431 DMCs were hypomethylated, while 3,771 were hypermethylated. Similarly, in the PHO:PC comparison, 3,434 DMCs were hypomethylated and 4,026 were hypermethylated. The PHO:PH comparison exhibited the highest number of modifications, with 5,922 hypomethylated and 6,330 hypermethylated. This balance in DMC distribution was also maintained when DMCs were analyzed according to their genomic regions (Fig. 2C).

DMCs located in promoters, gene bodies, and flanking regions were mapped to their corresponding genes. Genes containing DMCs indicative of an antagonistic effect between dietary MeHg and SeMet on cytosine methylation levels were identified. The Table 2 presents the five genes exhibiting opposing methylation trends between the PH:PC and PHO:PC comparisons. Among these, *methyltransferase-like 14* was particularly notable due to its methyltransferase activity.

Supplementary Table S3 highlights 800 genes where dietary MeHg and SeMet had an opposing influence on cytosine methylation. These genes displayed divergent methylation patterns in the PH:PC and PHO:PH comparisons, whereas no significant effect was observed in PHO:PC. Among these 800 genes, many were involved in key biological processes, including energy metabolism (particularly the respiratory chain and glucose metabolism), transcriptional regulation, immunity/inflammation, neurotransmission (Table 3).

3.3. Effects of dietary MeHg exposure, alone or combined with SeMet, on the brain transcriptome

Details of the RNA-seq alignment step can be found in **Supplementary Table S4**. A PCA was first performed on the top 500 high-variance genes to visualize sample clustering based on dietary exposure (Fig. 3A). The PCA did not reveal clear clusters by diet; however, fish exposed to both MeHg and SeMet showed less overlap with other groups compared to those exposed to MeHg alone or the control.

Gene expression changes were then quantified as log fold changes (LFCs) and compared across dietary treatments (PH:PC, PHO:PC, and PHO:PH) to assess differential expression. A total of 341 DEGs were identified and subsequently clustered using DBSCAN analysis based on their average expression in each dietary group. Two main clusters, C1 and C2, were distinguished (Fig. 3B). Cluster C1 contained 188 DEGs, following the expression trend PHO < PC < PH. Cluster C2 included 122 DEGs with the opposite trend: PH < PC < PHO (Fig. 3C). Additionally, 93 DEGs did not belong to any cluster.

Several DEGs in cluster C1 were associated with inflammation and immunity (e.g., immune cell migration) and energy metabolism (e.g., fatty acid β-oxidation, respiratory chain, glycolysis) (**Supplementary Table S5**). Notably, *hypoxia inducible factor 1 subunit alpha, like 2* was identified as a DEG in cluster C2. The full list of DEGs and their corresponding clusters is available in **Supplementary Table S5**.

A functional GSEA was conducted using three databases: GO terms, KEGG modules, and KEGG pathways, across the three pairwise comparisons (PH:PC, PHO:PC, and PHO:PH). Details of these analyses are presented in **Supplementary Tables S6, S7**, and **S8**, respectively.

The GSEA using GO terms identified 35 significantly affected pathways (2 downregulated, 33 upregulated) in the PH:PC comparison, 42 pathways (6 downregulated, 36 upregulated) in the PHO:PC comparison, and 10 pathways (all upregulated) in the PHO:PH comparison (**Supplementary Table S9**). Among these, the hormone activity pathway was differentially affected across conditions. Specifically, it was upregulated in PH:PC, downregulated in PHO:PH, and showed no significant change in PHO:PC.

Analysis using the KEGG module database revealed 18 significantly upregulated modules in PH:PC, predominantly related to energy metabolism, including glycolysis, the tricarboxylic acid (TCA) cycle, and the mitochondrial respiratory chain (**Supplementary Table S10**). In PHO:PC, seven modules were significantly affected (two downregulated, five upregulated). In PHO:PH, three modules were significantly downregulated. Notably, all commonly affected modules in PH:PC and PHO:PC were related to the mitochondrial respiratory chain and were

Table 2
DMCs showing opposite methylation trends under dietary MeHg (PH) versus MeHg + SeMet (PHO), relative to the control diet (PC).

Chromosome	Position	Region	Gene ID	Gene symbol	Gene name	methdiff PH:PC	methdiff PHO:PC	methdiff PHO:PH
NC_035097.1	2040522	Flank	110501052	LOC110501052	cGMP-inhibited 3′,5′-cyclic phosphodiesterase A-like	-20.48	25.27	45.75
NC_035089.1	26157016	Exon	110486063	LOC110486063	signal-induced proliferation-associated 1-like protein 2	25.95	-25.70	-51.64
NW_018630040.1	260	Flank	110519301	mettl14	methyltransferase like 14	26.90	-21.22	-48.13
NC_035087.1	29224941	Exon	110535572	LOC110535572	inhibin beta A chain-like	27.22	-23.31	-50.52
NC_035089.1	37226772	Intron	110486338	LOC110486338	protein shisa-9B-like	28.28	-21.90	-50.18

Table 3
DMCs exhibiting dietary MeHg-SeMet antagonism, localized within genes of interest.

Chromosome	Position	Region	Gene ID	Gene symbol	Gene name	Methylation (%) PH:PC	Methylation (%) PHO:PH
NC_035096.1	20995804	Flank	110499211	LOC110499211	cytochrome b-c1 complex subunit 2, mitochondrial	-58,92	55,47
NC_035085.1	41230792	Flank	110532257	LOC110532257	cytochrome c oxidase subunit 4 isoform 2, mitochondrial-like	-40,70	20,86
NC_035085.1	41230792	P1K	110532258	LOC110532258	cytochrome c oxidase subunit 4 isoform 2, mitochondrial-like	-40,70	20,86
NC_035098.1	43636936	P5K	110501918	LOC110501918	cytochrome c	-32,26	30,31
NC_035098.1	43636944	P5K	110501918	LOC110501918	cytochrome c	-23,93	25,09
NC_035079.1	54931057	Flank	110520174	LOC110520174	NADH dehydrogenase [ubiquinone] 1 alpha subcomplex subunit 10, mitochondrial-like, transcript variant X2	23,61	-32,05
NC_035077.1	10391259	Flank	110485648	LOC110485648	ATP synthase mitochondrial F1 complex assembly factor 1-like, transcript variant X1	28,34	-25,14
NC_035079.1	54931053	Flank	110520174	LOC110520174	NADH dehydrogenase [ubiquinone] 1 alpha subcomplex subunit 10, mitochondrial-like, transcript variant X2	33,56	-29,68
NC_035079.1	54931036	Flank	110520174	LOC110520174	NADH dehydrogenase [ubiquinone] 1 alpha subcomplex subunit 10, mitochondrial-like, transcript variant X2	38,23	-38,21
NC_035092.1	15582424	Flank	110491497	mrpl10	mitochondrial ribosomal protein L10	34,83	-28,08
NC_035102.1	16133447	Intron	110506482	LOC110506482	aryl hydrocarbon receptor nuclear translocator-like protein 1, transcript variant X2	-32,48	34,91
NC_035105.1	26093142	Flank	110509909	LOC110509909	V-type proton ATPase 116 kDa subunit a-like, transcript variant X1	-30,12	20,23
NC_035102.1	16128106	Exon	110506482	LOC110506482	aryl hydrocarbon receptor nuclear translocator-like protein 1, transcript variant X2	-21,37	22,43
NC_035092.1	52946360	Flank	110492374	LOC110492374	prostaglandin E synthase 3-like, transcript variant X2	48,72	-41,02
NC_035077.1	63667848	Flank	110527634	LOC110527634	nuclear factor NF-kappa-B p100 subunit-like, transcript variant X1	-50,36	30,37
NC_035077.1	63667878	Flank	110527634	LOC110527634	nuclear factor NF-kappa-B p100 subunit-like, transcript variant X1	-36,99	45,91
NC_035105.1	26093142	P5K	110509910	LOC110509910	NF-kappa-B inhibitor-like protein 1, transcript variant X2	-30,12	20,23
NC_035077.1	63667881	Flank	110527634	LOC110527634	nuclear factor NF-kappa-B p100 subunit-like, transcript variant X1	-28,25	22,30
NC_035088.1	22435993	Flank	110537273	LOC110537273	immunoglobulin-binding protein 1-like	-26,42	22,15
NC_035083.1	16184657	Exon	110527509	LOC110527509	immunoglobulin superfamily member 10-like	-25,43	24,11
NC_035088.1	77579495	P5K	110538565	LOC110538565	monocyte to macrophage differentiation factor-like, transcript variant X1	-23,61	20,77
NC_035087.1	42020534	Intron	110535028	LOC110535028	T-cell receptor gamma chain C region C10.5	-20,62	26,12
NC_035084.1	69831588	Flank	110530573	nfatc4	nuclear factor of activated T-cells 4	-20,18	28,81
NC_035094.1	12828609	Flank	100136113	tlr22	toll-like receptor 22	22,43	-25,34
NC_035094.1	12828609	Exon	110497090	LOC110497090	toll-like receptor 13	22,43	-25,34
NC_035093.1	67354757	Flank	110494740	LOC110494740	major histocompatibility complex class I-related gene protein-like, transcript variant X1	25,91	-22,39
NC_035091.1	57038799	P5K	110490557	LOC110490557	differentially expressed in FDCP 6-like	27,06	-21,68
NC_035093.1	40226152	Flank	110493220	LOC110493220	cysteinyl leukotriene receptor 2-like	34,39	-38,07
NC_035083.1	13789959	Intron	110527446	LOC110527446	gamma-aminobutyric acid receptor subunit beta-3-like, transcript variant X1	-31,46	25,84
NC_035083.1	13789959	Intron	110527447	LOC110527447	gamma-aminobutyric acid receptor subunit alpha-5-like	-31,46	25,84
NC_035088.1	48332547	Flank	110537751	LOC110537751	gamma-aminobutyric acid receptor subunit beta-2-like	-29,22	28,65
NC_035086.1	31950603	Flank	110533760	LOC110533760	glutamate receptor 3-like	-27,04	28,54
NC_035086.1	31950603	P1K	110533761	LOC110533761	glutamate receptor 3-like	-27,04	28,54
NC_035096.1	12787060	Intron	110498745	LOC110498745	glutamate receptor ionotropic, delta-1-like	-26,96	25,66
NC_035101.1	30804987	Exon	110505100	LOC110505100	gamma-aminobutyric acid receptor subunit alpha-2-like	-26,37	24,30
NC_035083.1	52555646	Intron	110528160	LOC110528160	metabotropic glutamate receptor 2-like	-22,44	25,48
NC_035088.1	31308905	Flank	110537507	LOC110537507	sodium- and chloride-dependent GABA transporter ine-like	21,09	-23,48
NC_035087.1	37457005	Intron	110535694	LOC110535694	glutamate receptor ionotropic, delta-2, transcript variant X1	22,06	-29,80

upregulated in both comparisons. In contrast, the β-oxidation acyl-CoA synthesis module (linked to energy metabolism) was downregulated in both PHO:PC and PHO:PH. Additionally, cholesterol biosynthesis, squalene 2,3-epoxide metabolism, and the gamma-aminobutyric acid (GABA) shunt were upregulated in PH:PC, downregulated in PHO:PC, and unaffected in PHO:PH.

The KEGG pathway-based GSEA identified 26 significantly affected pathways (3 downregulated, 23 upregulated) in PH:PC, 47 pathways (39 downregulated, 8 upregulated) in PHO:PC, and 45 pathways (42 downregulated, 3 upregulated) in PHO:PH (**Supplementary Table S11**). Several pathways related to energy metabolism, including glyoxylate and dicarboxylate metabolism, carbon metabolism, the TCA cycle, pyruvate metabolism, valine/leucine/isoleucine degradation, and propanoate metabolism, were upregulated in PH:PC, downregulated in PHO:PH, and unaffected in PHO:PC (Table 4). One pathway, fatty acid metabolism (involved in energy production via β-oxidation), was downregulated in both PHO:PC and PHO:PH but upregulated in PH:PC (Table 4).

4. Discussion

4.1. SeMet antagonizes the molecular influences of dietary MeHg: methylomic and transcriptomic evidence

SAM levels, a key marker of methylation potential, were not altered by MeHg alone, consistent with previous studies in zebrafish exposed to dietary MeHg (10 μg/g) for 47 days (Olsvik et al., 2014). In contrast, co-exposure with SeMet decreased brain SAM levels. Such an effect of

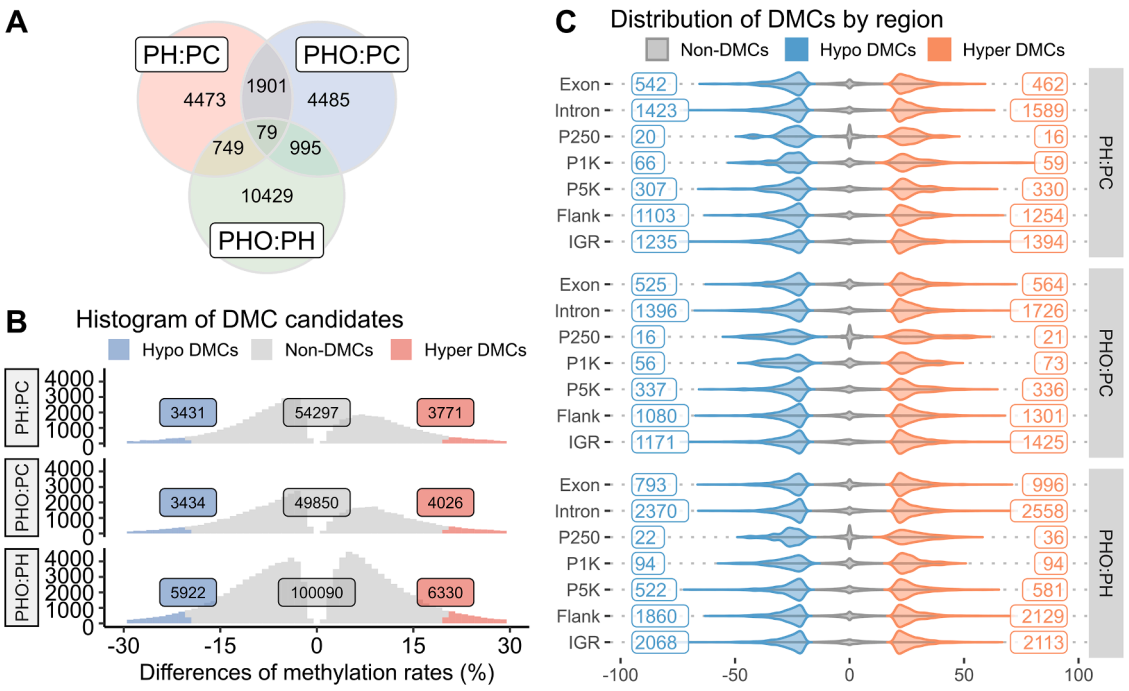

Fig. 3. A: PCA shows top 500 high variance genes of the RNA sequencing analysis in brain of rainbow trout (n = 6) after six months of feeding; B and C: DBSCAN analysis of the pooled DEGs (adjusted p-value ≤ 0.1) and clustered based on their average expressions, two clusters were identified C1 (average expression pattern: PHO < PC < PH) and C2 (average expression pattern: PH < PC < PHO).

Table 4
Enriched KEGG pathways identified by GSEA that exhibited dietary MeHg–SeMet interaction.

Pathway	KEGG ID	GSEA		
		PH:PC	PHO:PC	PHO:PH
Fatty acid metabolism	omy01212	1.74***	-1.51*	-1.86***
Butanoate metabolism	omy00650	1.85***	-	-1.75**
Carbon metabolism	omy01200	1.98***	-	-1.46*
Citrate cycle (TCA cycle)	omy00020	2.26***	-	-1.79**
Pyruvate metabolism	omy00620	2.01***	-	-1.54*
Valine, leucine and isoleucine degradation	omy00280	1.91***	-	-1.94***
Propanoate metabolism	omy00640	1.95***	-	-1.86**
Glyoxylate and dicarboxylate metabolism	omy00630	1.80**	-	-1.64*
Glycine, serine and threonine metabolism	omy00260	1.58*	-	-1.59*

NES (normalized enrichment score) for each pathway was given, a positive NES indicated an up-regulation of the pathway whereas a negative NES indicated a down-regulation. The significance of the affected pathway was given by the adjusted p-value < 0.001 (***), < 0.01 (**), < 0.05 (*). The symbol "-" means that the pathway was not identified as significantly affected in the corresponding pairwise comparison.

SeMet was also observed in the liver of broodstock rainbow trout exposed for six months to diets containing 0.7 μg/g Se, primarily supplied as hydroxy-SeMet (Wischhusen et al., 2020). The reduction in SAM levels did not translate into a lower number of DMCs or altered distribution of hypo- and hypermethylated cytosines in the PH:PC and PHO:PC comparisons, suggesting that SAM, a methyl donor for multiple processes (Loenen, 2018) was utilized in Se-related processes other than DNA methylation.

Approximately 800 DMCs showed antagonistic methylation patterns when MeHg was administered alone versus in combination with SeMet. Functional annotation associated these DMCs to inflammation-related genes. Previous studies have demonstrated the influence of SeMet on cytosine methylation in genes associated with inflammation and immunity in the liver of broodstock rainbow trout, suggesting a potential immunostimulatory role of Se (Wischhusen et al., 2020). Recent research on MeHg-induced DNA methylation changes in human blood also identified methylation alterations in genes related to inflammation and autoimmunity (Weinhouse et al., 2022). Furthermore, our previous study highlighted the counteractive effects of SeMet on MeHg-induced pro-inflammatory responses in rainbow trout plasma (Bidon et al., 2023). Therefore, the observed antagonism between dietary MeHg and SeMet could be interpreted as a mechanism through which SeMet modulates MeHg-associated molecular signatures related to neuro-inflammatory processes, as previously reported in brain of mice treated with intraperitoneal injections of MeHg (Hwang et al., 2011). Furthermore, the current study revealed that DMCs exhibiting antagonistic behavior between SeMet and MeHg were associated with genes involved in neurotransmitter systems, especially the glutamatergic system. This neurotransmitter system is reported to be dysregulated in the presence of MeHg and is proposed as a mechanism through which MeHg induces neurotoxicity (Aschner et al., 2007). Hence, the antagonistic impact of SeMet on cytosine methylation in genes related to the glutamatergic system could represent a molecular mechanism through which SeMet modulates pathways known to be involved in MeHg-induced neurotoxicity. Lastly, the DMCs displaying antagonistic behavior between SeMet and MeHg were also linked to processes related to energy metabolism, a phenomenon that was similarly observed at a transcriptomic level.

In fact, the GSEA analysis, particularly using the KEGG pathway database, highlighted a significant interaction between dietary MeHg and SeMet on pathways associated with energy metabolism, including glycolysis, oxidative phosphorylation, the TCA cycle, and the respiratory chain. Notably, all these pathways were upregulated in fish exposed to dietary MeHg. This observation aligns with previous studies, such as in zebrafish exposed to dietary MeHg (13.5 μg/g) for 25 days, where MeHg significantly influenced gene expression related to energy metabolism in muscle, leading to an upregulation of genes associated with glycolysis and the mitochondrial respiratory chain (Cambier et al., 2010). Similarly, in Atlantic cod (*Gadus morhua*) exposed to dietary MeHg (0.5-2

μg/g) for 14 days, an upregulation of gene expression related to glycolysis and fatty acid metabolism was observed in the liver (Yadetie et al., 2013). These findings corroborate our results and they reinforce the hypothesis that MeHg disrupts energy metabolism. Such alterations in energetic pathways may reflect an adaptive metabolic response to chronic MeHg exposure, rather than overt mitochondrial dysfunction. However, when fish were co-exposed to dietary SeMet and MeHg, these pathways returned to levels comparable to the control group, suggesting an antagonistic interaction between SeMet and MeHg at the molecular level. A proteomic study in zebrafish brains exposed to dietary SeMet and MeHg (5 μg/g and 10 μg/g, respectively) supports our finding, revealing an antagonistic effect on proteins involved in glycolysis, oxidative phosphorylation, the TCA cycle, and mitochondrial function (Rasinger et al., 2017).

Our previous work conducted on fish originating from the same feeding trial as the present study demonstrated that dietary MeHg exposure induced adverse effects at short term. Indeed, after 21 days of exposure, rainbow trout fed a MeHg-supplemented diet exhibited a significant reduction in growth, concomitant with increased circulating pro-inflammatory cytokines (Bidon et al., 2023). In contrast, after 6 months of feeding, trout fed the same diet no longer displayed impaired growth or elevated inflammatory markers. This apparent recovery was associated with a marked decrease in Hg retention compared to fish exposed for 21 days, suggesting the implementation of compensatory or detoxification mechanisms over time (Bidon et al., 2023). Consistently, a second study investigating Hg and Se biokinetics in rainbow trout organs reported reduced Hg bioaccumulation after 6 months than after only 21 days of exposure (Marchán-Moreno et al., 2024). Furthermore, changes in Hg biomolecular fraction, particularly in the kidney, were observed between 21 days and 6 months, indicating a progressive redistribution of Hg from high- to low-molecular-weight binding molecules (El Hanafi et al., 2024). These findings were interpreted by the authors as evidence of adaptive detoxification strategies in trout subjected to chronic MeHg exposure. Together, these results strongly suggest that physiological responses to MeHg are time-dependent. While MeHg induces clear adverse effects at early exposure stages, prolonged exposure appears to trigger putative adaptive responses that mitigate MeHg influences. In this context, the molecular alterations reported in the present study after 6 months of exposure are more likely reflective of adaptive or compensatory mechanisms rather than direct toxic effects. Importantly, our previous study also showed that dietary SeMet supplementation mitigated the transient growth impairment induced by MeHg after 21 days of exposure, although it did not significantly affect pro-inflammatory cytokine levels (Bidon et al., 2023). This protective effect was not detectable after 6 months, likely due to the masking effect of long-term putative adaptive response to MeHg. Therefore, the molecular differences observed between fish fed MeHg alone and those fed MeHg concomitantly with SeMet may reflect a modulatory effect of SeMet on the molecular compensatory mechanisms implemented to cope with chronic MeHg exposure.

Although SeMet significantly increased brain Se concentration, confirming its bioavailability, the molecular antagonism described above was not mediated by changes in Hg bioaccumulation. In fact, in the present study, SeMet supplementation did not reduce brain Hg levels, contrasting with results in zebrafish fed higher MeHg and SeMet concentrations (10 μg/g MeHg and 5 μg/g SeMet), where SeMet supplementation reduced brain Hg concentration by 35% (Rasinger et al., 2017). The discrepancy likely reflects the lower dietary exposure levels used in the present study (2 μg/g and 1.5 μg/g, respectively). Even though, it should be underlined that another study conducted on fish originating from the same feeding trial consistently reported no significant effect of dietary SeMet, when provided concomitantly with MeHg, on total Hg bioaccumulation at both whole-body and organ levels (Bidon et al., 2023; Marchán-Moreno et al., 2024). This observation is consistent with our results showing that Hg concentrations in the brain were not significantly affected by SeMet supplementation. The lack of influence of dietary SeMet on Hg bioaccumulation has also been reported in rainbow trout exposed for 3 months to dietary MeHg (0.2 ppm) and SeMet (5 ppm), where SeMet did not alter Hg accumulation in edible tissues (Ribeiro et al., 2022). Importantly, antagonistic interactions between Se and Hg do not necessarily translate into a reduction of total Hg concentrations, but may instead involve changes in Hg biomolecular distribution. In line with this hypothesis, El Hanafi et al. (2024) demonstrated that dietary co-exposure to MeHg and SeMet induced marked changes in Hg biomolecular partitioning in the liver, despite similar levels of total hepatic Hg accumulation (Marchán-Moreno et al., 2024). In that study, Hg was identified as being associated with metallothioneins and GSH in fish tissues, two key molecules involved in MeHg detoxification processes. The brain represents a particularly challenging matrix for speciation analyses due to its limited tissue mass and the low concentrations of both Hg and Se compared to other organs, which strongly constrain analytical sensitivity. Consequently, the identification of Hg-containing complexes in the brain relies partly on indirect evidence derived from chromatographic patterns observed in other tissues. Therefore, a redistribution of Hg towards alternative biomolecular pools in the brain under SeMet supplementation cannot be excluded, but requires further investigation to be conclusively demonstrated. From a mechanistic perspective, GSH is known to play a central role in MeHg detoxification and excretion (Wang et al., 2017), while metallothioneins have been reported to confer protection against MeHg-induced neurotoxicity through their chelating properties, without necessarily reducing total Hg accumulation in neural tissues (West et al., 2008). In addition, the blood–brain barrier, due to its low permeability, may limit Hg efflux from the brain, thereby reducing the apparent effect of dietary SeMet on Hg bioaccumulation. Although not statistically significant, a reduction of approximately 18% in brain Hg concentration was observed in fish co-exposed to MeHg and SeMet compared to fish exposed to MeHg alone, suggesting a potential trend toward a decreased Hg burden. Finally, a study on catfish (*Clarias gariepinus*) exposed to a concentration of 0.12 ppm of Hg concomitantly with 0.1 ppm of Se for 30 days found that Se had no influence on Hg bioaccumulation in the fish testicles, but did have a protective effect on the fish reproductive system exposed to Hg (Ibrahim et al., 2019). Collectively, these findings support the hypothesis that dietary SeMet may exert protective effects primarily by modulating Hg biomolecular distribution rather than by reducing total Hg bioaccumulation in the brain. Such mechanisms should be taken into account when interpreting molecular differences observed in fish brain despite comparable Hg concentrations across treatments.

4.2. *Hif1al2: a key potential target in the SeMet–MeHg interaction affecting energy metabolism*

Hg and Se interactions may indirectly influence hypoxia inducible factors (HIFs) level through their effects on oxygen transport. Previous bioaccumulation studies conducted on fish from the same feeding trial showed that a major fraction of Hg accumulated in the blood (Marchán-Moreno et al., 2024). More recently, chromatographic analyses suggested that Hg in blood is largely associated with hemoglobin (El Hanafi et al., 2024). Given the central role of hemoglobin in oxygen transport, it has been proposed that Hg binding may impair hemoglobin oxygen-binding capacity (Piscopo et al., 2020). Dietary SeMet supplementation may modulate this process by altering Hg distribution in the bloodstream. Organic Se has been shown to increase hepatic expression of selenoprotein P in rainbow trout (Pacitti et al., 2016), a key plasmatic selenoprotein responsible for Se transport (Saito, 2021). Because Hg exhibits a higher binding affinity for selenol groups present in selenoproteins than for thiol groups found in hemoglobin (Wang et al., 2011), SeMet supplementation could favor the redistribution of Hg from hemoglobin toward selenoproteins. A redistribution of Hg biomolecular fraction under the influence of SeMet dietary addition has been previously observed in the liver of fish from the same experimental set (El

Hanafi et al., 2024). HIF transcription factors are highly sensitive to changes in oxygen availability and play a central role in the regulation of cellular energy metabolism (Taylor and Scholz, 2022). Their expression varies depending on HIF family member, tissue type, exposure duration, and hypoxia severity (Jaśkiewicz et al., 2022; Murphy and Rees, 2024). In this context, alterations in oxygen transport induced by Hg exposure, and its potential mitigation by SeMet through Hg redistribution, could contribute to the modulation of the expression of the transcript encoding *hypoxia-inducible factor 1 subunit alpha-like 2 (hif1al2)* found as differentially expressed in our results, lower in the PH diet and higher in brain of fish fed a PHO diet. Therefore, *hif1al2* emerges as a plausible molecular target linking Hg–Se interactions to the molecular regulation of energetic pathways observed in the present study.

Although the transcript name *hif1al2* suggests a paralogous relationship with the transcript encoding HIF-1α in rainbow trout, NCBI Gene and Alliance of Genome Resources indicate that *hif1al2* in zebrafish (a close taxon to rainbow trout) is the ortholog of the human gene *hypoxia inducible factor 3 subunit alpha* (*HIF3A*). The orthology–function conjecture states that orthologous genes are generally preferred when making assumptions about gene function across species (Chen and Zhang, 2012). HIFs constitute a family of transcription factors with several members whose primary function is to regulate energy metabolism (Semenza, 2012); unfortunately, HIF-3α remains the least well characterized (Ravenna et al., 2016). Studies using *in vitro* approaches of murine pre-adipocytes, human adipocyte cell lines, and an *in vivo* murine model showed that HIF-3α influenced the energetic metabolism. In fact, the authors showed that the inhibition of HIF-3α leads to increased energy metabolism with enhanced lipolysis, mitochondrial respiration, and acetyl-CoA metabolism (Kulyté et al., 2020; Cuomo et al., 2022). These observations are consistent with our results, where the lowest *hif1al2* expression was measured in the brains of fish fed MeHg-supplemented diets, coinciding with enrichment of energy metabolism pathways. Conversely, the highest *hif1al2* expression was observed in fish exposed to both MeHg and SeMet where energy metabolism pathways were downregulated, compared to MeHg fed fish.

4.3. Oxidative stress as a potential regulator of *hif1al2* transcript levels?

Oxidative stress is a mechanism reported to influence HIF-1α levels (Movafagh et al., 2015), a feature proposed to be at the interface between HIF-1α and MeHg interplay (Chang et al., 2019). An *in vivo* study in rats and an *in vitro* study in rat astrocytes, showed that MeHg reduced HIF-1α protein levels without altering its mRNA expression (Chang et al., 2019). Moreover, Chang et al. (2019) demonstrated that *hif-1α* overexpression provided neuroprotection against MeHg toxicity, and suggested a link between MeHg oxidative stress induction and HIF-1α regulation. Given the well-documented antioxidant properties of SeMet in fish (Li et al., 2023), its presence in the diet may have mitigated oxidative stress induced by MeHg, thereby increasing *hif1al2* transcript levels. However, it is important to emphasize that neither our transcriptomic analysis nor the measurements of GSH metabolites provided direct evidence of overt oxidative stress in rainbow trout brains exposed to dietary MeHg at the levels tested. The glutathione system is a primary target of MeHg neurotoxicity, typically leading to reduced GSH levels and impaired antioxidant capacity (Stringari et al., 2008). In this study, no significant decrease in GSH levels was observed. Nonetheless, MeHg can induce oxidative stress even without major changes in GSH levels, likely due to its impact on alternative antioxidant mechanisms (Wei et al., 2021). Therefore, further investigations assessing additional oxidative stress markers are warranted to clarify the potential role of oxidative stress in regulating *hif1al2* transcript level in the brains of rainbow trout.

Moreover, it should be emphasized that, despite some overlaps between the molecular targets of HIF-1α and HIF-3α observed in zebrafish (Zhang et al., 2014), which might indicate functional similarity between these two HIF family members. The extrapolation of the observations between HIF-1α and MeHg and the molecular mechanisms involved in HIF-1α degradation and how it can apply to HIF-3α should be interpreted with caution. To date, studies investigating HIF-3α and MeHg interactions are lacking. Moreover, the mechanism by which HIF-3α is degraded is still not documented.

5. Conclusion

Our findings provide new insights into the interplay between DNA methylation and transcript levels, shedding light on the molecular responses associated with chronic dietary exposure to of MeHg and its interaction with SeMet in the brains of rainbow trout. Our data indicate that SeMet modulates MeHg-associated molecular alterations, particularly in DNA methylation patterns of genes related to the glutamatergic system and inflammation/immunity. At the transcriptomic level, significant interactions between MeHg and SeMet were observed in pathways related to energy metabolism, with *hif1al2* (predicted to be the human *HIF3A* ortholog based on the zebrafish data), as a potential mediator of this interaction. Together, these results suggest that SeMet influences early or compensatory molecular responses to MeHg exposure, even in the absence of overt neurotoxic symptoms. Further investigations focusing on HIF-3α function and downstream pathways are warranted to better understand the mechanisms underlying SeMet-MeHg interaction in fish brains.

Data availability: Data will be made available on request.

CRediT authorship contribution statement

Marius Bidon: Writing – review & editing, Writing – original draft, Investigation, Formal analysis, Data curation, Conceptualization. **Takaya Saito:** Writing – review & editing, Visualization, Methodology, Investigation, Formal analysis, Data curation. **Kaja H. Skjaerven:** Writing – review & editing, Supervision, Methodology. **Philip Antony Jesu Prabhu:** Writing – review & editing, Supervision, Funding acquisition, Conceptualization. **Cécile Heraud:** Formal analysis. **Jérôme Roy:** Writing – review & editing, Supervision. **Claudia Marchán-Moreno:** Formal analysis. **Zoyne Pedrero-Zayas:** Writing – review & editing, Funding acquisition, Conceptualization. **Stéphanie Fontagné-Dicharry:** Writing – review & editing, Supervision, Conceptualization.

Declaration of competing interest

The authors declare that they have no known competing financial interests or personal relationships that could have appeared to influence the work reported in this paper.

Acknowledgements

This study was supported by I-site E2S: Energy and Environment Solutions from the University of Pau and Pays de l'Adour (UPPA), under contract 2020–32 (M.B., PhD fellowship). The authors gratefully acknowledge financial support from the Agence Nationale de la Recherche (MERSEL Project, ANR-18-CE34-0004–01) and the Institute of Marine Research, Norway (TuneSel Project, no 15745). This project also received funding from the European Union's Horizon 2020 research and innovation programme under the Marie Skłodowska-Curie Grant Agreement no 101007962. The authors would like to express their gratitude to Orffa (Breda, The Netherlands) for kindly providing selenomethionine. They also extend their sincere thanks to F. Terrier and A. Lanuque, and F. Sandres for their assistance in diet preparation and fish care, as well as to A. Surget, L. Larroquet, K. Dias, V. Véron, M. Marchand, F. Vallée, and A. Braun for their valuable help during sample collection.

Supplementary materials

Supplementary material associated with this article can be found, in the online version, at doi:10.1016/j.aquatox.2026.107706.

Data availability

Data will be made available on request.

References

Akalin, A., Kormaksson, M., Li, S., Garrett-Bakelman, F.E., Figueroa, M.E., Melnick, A., Mason, C.E., 2012. MethylKit: a comprehensive R package for the analysis of genome-wide DNA methylation profiles. Genome Biol. 13, R87. https://doi.org/10.1186/gb-2012-13-10-R87.

Aschner, M., Syversen, T., Souza, D.O., Rocha, J.B.T., Farina, M., 2007. Involvement of glutamate and reactive oxygen species in methylmercury neurotoxicity. Braz. J. Med. Biol. Res. 40, 285–291. https://doi.org/10.1590/S0100-879X2007000300001.

Baldissera, M.D., Souza, C.F., da Silva, A.S., Henn, A.S., Flores, E.M.M., Baldisserotto, B., 2020. Diphenyl diselenide dietary supplementation alleviates behavior impairment and brain damage in grass carp (*Ctenopharyngodon idella*) exposed to methylmercury chloride. Comp. Biochem. Physiol. C-Toxicol. Pharmacol. 229. https://doi.org/10.1016/j.cbpc.2019.108674.

Barbosa, R.V., Point, D., Médieu, A., Allain, V., Gillikin, D.P., Couturier, L.I.E., Munaron, J.-M., Roupsard, F., Lorrain, A., 2022. Mercury concentrations in tuna blood and muscle mirror seawater methylmercury in the Western and Central Pacific Ocean. Mar. Pollut. Bull. 180, 113801. https://doi.org/10.1016/j.marpolbul.2022.113801.

Basu, N., Head, J., Nam, D.-H., Pilsner, J.R., Carvan, M.J., Chan, H.M., Goetz, F.W., Murphy, C.A., Rouvinen-Watt, K., Scheuhammer, A.M., 2013. Effects of methylmercury on epigenetic markers in three model species: mink, chicken and yellow perch. Comp. Biochem. Physiol. C. Toxicol. Pharmacol. 157, 322–327. https://doi.org/10.1016/j.cbpc.2013.02.004.

Berg, K., Puntervoll, P., Valdersnes, S., Goksøyr, A., 2010. Responses in the brain proteome of Atlantic cod (*Gadus morhua*) exposed to methylmercury. Aquat. Toxicol. 100, 51–65. https://doi.org/10.1016/j.aquatox.2010.07.008.

Berntssen, M.H.G., Aatland, A., Handy, R.D., 2003. Chronic dietary mercury exposure causes oxidative stress, brain lesions, and altered behaviour in Atlantic salmon (*Salmo salar*) parr. Aquat. Toxicol. 65, 55–72. https://doi.org/10.1016/S0166-445X(03)00104-8.

Berntssen, M.H.G., Betancor, M., Caballero, M.J., Hillestad, M., Rasinger, J., Hamre, K., Sele, V., Amlund, H., Ørnsrud, R., 2018. Safe limits of selenomethionine and selenite supplementation to plant-based Atlantic salmon feeds. Aquaculture 495, 617–630. https://doi.org/10.1016/j.aquaculture.2018.06.041.

Bidon, M., Philip, A.J.P., Braun, A., Herman, A., Roy, J., Pedrero-Zayas, Z., Fontagné-Dicharry, S., 2023. Interaction between dietary selenium and methylmercury on growth performance, deposition and health parameters in rainbow trout fed selenium-rich tuna-based diets or selenium-poor plant-based diets. Aquaculture 572, 739550. https://doi.org/10.1016/j.aquaculture.2023.739550.

Bjerregaard, P., Fjordside, S., Hansen, M.G., Petrova, M.B., 2011. Dietary selenium reduces retention of methyl mercury in freshwater fish. Env. Sci. Technol. 45, 9793–9798. https://doi.org/10.1021/es202565g.

Cambier, S., Gonzalez, P., Durrieu, G., Maury-Brachet, R., Boudou, A., Bourdineaud, J.-P., 2010. Serial analysis of gene expression in the skeletal muscles of zebrafish fed with a methylmercury-contaminated diet. Env. Sci. Technol. 44, 469–475. https://doi.org/10.1021/es901980t.

Cardoso, O., Puga, S., Brandão, F., Canário, J., O'Driscoll, N.J., Santos, M.A., Pacheco, M., Pereira, P., 2017. Oxidative stress profiles in brain point out a higher susceptibility of fish to waterborne divalent mercury compared to dietary organic mercury. Mar. Pollut. Bull. 122, 110–121. https://doi.org/10.1016/j.marpolbul.2017.06.029.

Caudill, M.A., Wang, J.C., Melnyk, S., Pogribny, I.P., Collins, M.D., Santos-Guzman, J., Swendseid, M.E., Cogger, E.A., James, S.J., Jernigan, S., 2001. Intracellular S-adenosylhomocysteine concentrations predict global DNA hypomethylation in tissues of methyl-deficient cystathionine β-synthase heterozygous mice. J. Nutr. 131, 2811–2818. https://doi.org/10.1093/jn/131.11.2811.

Chang, J., Yang, B., Zhou, Y., Yin, C., Liu, T., Qian, H., Xing, G., Wang, S., Li, F., Zhang, Y., Chen, D., Aschner, M., Lu, R., 2019. Acute methylmercury exposure and the hypoxia-inducible factor-1α signaling pathway under normoxic conditions in the rat brain and astrocytes in vitro. Env. Health Perspect. 127, 127006. https://doi.org/10.1289/EHP5139.

Chen, X., Zhang, J., 2012. The ortholog conjecture is untestable by the current gene ontology but is supported by RNA sequencing data. PLoS. Comput. Biol. 8, e1002784. https://doi.org/10.1371/journal.pcbi.1002784.

Cressey, P., Miles, G., Saunders, D., Pearson, A.J., 2020. Mercury, methylmercury and long-chain polyunsaturated fatty acids in selected fish species and comparison of approaches to risk-benefit analysis. Food Chem. Toxicol. 146, 111788. https://doi.org/10.1016/j.fct.2020.111788.

Culbreth, M., Aschner, M., 2019. Methylmercury epigenetics. Toxics. 7, 56. https://doi.org/10.3390/toxics7040056.

Cuomo, F., Dell'Aversana, C., Chioccarelli, T., Porreca, V., Manfrevola, F., Papulino, C., Carafa, V., Benedetti, R., Altucci, L., Cobellis, G., Cobellis, G., 2022. HIF3A inhibition triggers browning of white adipocytes via metabolic rewiring. Front. Cell Dev. Biol. 9. https://doi.org/10.3389/fcell.2021.740203.

Dobin, A., Davis, C.A., Schlesinger, F., Drenkow, J., Zaleski, C., Jha, S., Batut, P., Chaisson, M., Gingeras, T.R., 2013. STAR: ultrafast universal RNA-seq aligner. Bioinformatics. 29, 15–21. https://doi.org/10.1093/bioinformatics/bts635.

El Hanafi, K., Fernández-Bautista, T., Ouerdane, L., Corns, W.T., Bueno, M., Fontagné-Dicharry, S., Amouroux, D., Pedrero, Z., 2024. Exploring mercury detoxification in fish: the role of selenium from tuna byproduct diets for sustainable aquaculture. J. Hazard. Mater., 135779 https://doi.org/10.1016/j.jhazmat.2024.135779.

Ester, M., Kriegel, H.-P., Sander, J., Xu, X., 1996. A density-based algorithm for discovering clusters in large spatial databases with noise. In: Proceedings of the Second International Conference on Knowledge Discovery and Data Mining, pp. 226–231. https://doi.org/10.5555/3001460.3001507.

Ewels, P., Magnusson, M., Lundin, S., Käller, M., 2016. MultiQC: summarize analysis results for multiple tools and samples in a single report. Bioinformatics. 32, 3047–3048. https://doi.org/10.1093/bioinformatics/btw354.

Fernandes Azevedo, B., Barros Furieri, L., Peçanha, F.M., Wiggers, G.A., Frizera Vassallo, P., Ronacher Simões, M., Fiorim, J., Rossi de Batista, P., Fioresi, M., Rossoni, L., Stefanon, I., Alonso, M.J., Salaices, M., Valentim Vassallo, D., 2012. Toxic effects of mercury on the cardiovascular and central nervous systems. Biomed. Res. Int. 2012, 949048. https://doi.org/10.1155/2012/949048.

Fernández-Bautista, T., Gómez-Gómez, B., Gracia-Lor, E., Pérez-Corona, T., Madrid, Y., 2024. Selenium Health Benefit values and Hg and Se speciation studies for elucidating the quality and safety of highly consumed fish species and fish-derived products. Food Chem. 435, 137544. https://doi.org/10.1016/j.foodchem.2023.137544.

Hahsler, M., Piekenbrock, M., Doran, D., 2019. Dbscan: fast density-based clustering with R. J. Stat. Softw. 91, 1. https://doi.org/10.18637/jss.v091.i01.

Hall, B.D., Bodaly, R.A., Fudge, R.J.P., Rudd, J.W.M., Rosenberg, D.M., 1997. Food as the dominant pathway of methylmercury uptake by fish. Water. Air. Soil. Pollut. 100, 13–24. https://doi.org/10.1023/A:1018071406537.

Horowitz, H.M., Jacob, D.J., Zhang, Y., Dibble, T.S., Slemr, F., Amos, H.M., Schmidt, J. A., Corbitt, E.S., Marais, E.A., Sunderland, E.M., 2017. A new mechanism for atmospheric mercury redox chemistry: implications for the global mercury budget. Atmos. Chem. Phys. 17, 6353–6371. https://doi.org/10.5194/acp-17-6353-2017.

Hsu-Kim, H., Kucharzyk, K.H., Zhang, T., Deshusses, M.A., 2013. Mechanisms regulating mercury bioavailability for methylating microorganisms in the aquatic environment: a critical review. Env. Sci. Technol. 47, 2441–2456. https://doi.org/10.1021/es304370g.

Hwang, G.-W., Lee, J.-Y., Ryoke, K., Matsuyama, F., Kim, J.-M., Takahashi, T., Naganuma, A., 2011. Gene expression profiling using DNA microarray analysis of the cerebellum of mice treated with methylmercury. J. Toxicol. Sci. 36, 389–391. https://doi.org/10.2131/jts.36.389.

Ibrahim, A.T.A., Banaee, M., Sureda, A., 2019. Selenium protection against mercury toxicity on the male reproductive system of *Clarias gariepinus*. Comp. Biochem. Physiol. C. Toxicol. Pharmacol. 225, 108583. https://doi.org/10.1016/j.cbpc.2019.108583.

Jaśkiewicz, M., Moszyńska, A., Króliczewski, J., Cabaj, A., Bartoszewska, S., Charzyńska, A., Gebert, M., Dąbrowski, M., Collawn, J.F., Bartoszewski, R., 2022. The transition from HIF-1 to HIF-2 during prolonged hypoxia results from reactivation of PHDs and HIF1A mRNA instability. Cell Mol. Biol. Lett. 27, 109. https://doi.org/10.1186/s11658-022-00408-7.

Jeong, H., Ali, W., Zinck, P., Souissi, S., Lee, J.-S., 2024. Toxicity of methylmercury in aquatic organisms and interaction with environmental factors and coexisting pollutants: a review. Sci. Total Env. 943, 173574. https://doi.org/10.1016/j.scitotenv.2024.173574.

Kanehisa, M., Goto, S., 2000. KEGG: kyoto encyclopedia of genes and genomes. Nucleic. Acids. Res. 28, 27–30. https://doi.org/10.1093/nar/28.1.27.

Klaper, R., Rees Christopher, B., Drevnick, P., Weber, D., Sandheinrich, M., Carvan Michael, J., 2006. Gene expression changes related to endocrine function and decline in reproduction in fathead minnow (*Pimephales promelas*) after dietary methylmercury exposure. Env. Health Perspect. 114, 1337–1343. https://doi.org/10.1289/ehp.8786.

Krueger, F., Andrews, S.R., 2011. Bismark: a flexible aligner and methylation caller for Bisulfite-Seq applications. Bioinformatics. 27, 1571–1572. https://doi.org/10.1093/bioinformatics/btr167.

Kulyté, A., Lundbäck, V., Lindgren, C.M., Luan, J.a., Lotta, L.A., Langenberg, C., Arner, P., Strawbridge, R.J., Dahlman, I., 2020. Genome-wide association study of adipocyte lipolysis in the GENetics of adipocyte lipolysis (GENiAL) cohort. Mol. Metab. 34, 85–96. https://doi.org/10.1016/j.molmet.2020.01.009.

Lamborg, C.H., Hammerschmidt, C.R., Bowman, K.L., Swarr, G.J., Munson, K.M., Ohnemus, D.C., Lam, P.J., Heimbürger, L.-E., Rijkenberg, M.J.A., Saito, M.A., 2014. A global ocean inventory of anthropogenic mercury based on water column measurements. Nature 512, 65–68. https://doi.org/10.1038/nature13563.

Lavoie, R.A., Jardine, T.D., Chumchal, M.M., Kidd, K.A., Campbell, L.M., 2013. Biomagnification of mercury in aquatic food webs: a worldwide meta-analysis. Env. Sci. Technol. 47, 13385–13394. https://doi.org/10.1021/es403103t.

Lawrence, M., Huber, W., Pagès, H., Aboyoun, P., Carlson, M., Gentleman, R., Morgan, M.T., Carey, V.J., 2013. Software for computing and annotating genomic ranges. PLoS. Comput. Biol. 9, e1003118. https://doi.org/10.1371/journal.pcbi.1003118.

Li, Z.-M., Wang, X.-L., Jin, X.-M., Huang, J.-Q., Wang, L.-S., 2023. The effect of selenium on antioxidant system in aquaculture animals. Front. Physiol. 14, 1153511. https://doi.org/10.3389/fphys.2023.1153511.

Liao, Y., Smyth, G.K., Shi, W., 2014. featureCounts: an efficient general purpose program for assigning sequence reads to genomic features. Bioinformatics. 30, 923–930. https://doi.org/10.1093/bioinformatics/btt656.

Liu, Q., Basu, N., Goetz, G., Jiang, N., Hutz, R.J., Tonellato, P.J., Carvan, M.J., 2013. Differential gene expression associated with dietary methylmercury (MeHg) exposure in rainbow trout (*Oncorhynchus mykiss*) and zebrafish (*Danio rerio*). Ecotoxicology. 22, 740–751. https://doi.org/10.1007/s10646-013-1066-9.

Loenen, W.A.M., 2018. S-adenosylmethionine metabolism and aging. In: Moskalev, A., Vaiserman, A.M. (Eds.), Epigenetics of Aging and Longevity. Academic Press, pp. 59–93. https://doi.org/10.1016/B978-0-12-811060-7.00003-6.

Love, M.I., Huber, W., Anders, S., 2014. Moderated estimation of fold change and dispersion for RNA-seq data with DESeq2. Genome Biol. 15, 550. https://doi.org/10.1186/s13059-014-0550-8.

Marchán-Moreno, C., Queipo-Abad, S., Corns, W.T., Bueno, M., Pannier, F., Amouroux, D., Fontagné-Dicharry, S., Pedrero, Z., 2024. Assessment of dietary selenium and its role in mercury fate in cultured fish rainbow trout with two sustainable aquafeeds. Food Chem., 138865 https://doi.org/10.1016/j.foodchem.2024.138865.

McCarrey, J.R., 2003. Epigenetic mechanisms regulating gene expression. In: Krawetz, S. A., Womble, D.D. (Eds.), Introduction to Bioinformatics. Humana Press, pp. 123–139. https://doi.org/10.1007/978-1-59259-335-4_6.

Mellingen, R.M., Myrmel, L.S., Rasinger, J.D., Lie, K.K., Bernhard, A., Madsen, L., Nøstbakken, O.J., 2022. Dietary selenomethionine reduce mercury tissue levels and modulate methylmercury induced proteomic and transcriptomic alterations in hippocampi of adolescent BALB/c mice. Int. J. Mol. Sci. 23, 12242. https://doi.org/10.3390/ijms232012242.

Mille, T., Bisch, A., Caill-Milly, N., Cresson, P., Deborde, J., Gueux, A., Morandeau, G., Monperrus, M., 2021. Distribution of mercury species in different tissues and trophic levels of commonly consumed fish species from the south Bay of Biscay (France). Mar. Pollut. Bull. 166, 112172. https://doi.org/10.1016/j.marpolbul.2021.112172.

Moore, L.D., Le, T., Fan, G., 2013. DNA methylation and its basic function. Neuropsychopharmacology 38, 23–38. https://doi.org/10.1038/npp.2012.112.

Movafagh, S., Crook, S., Vo, K., 2015. Regulation of hypoxia-inducible factor-1a by reactive oxygen species: new developments in an old debate. J. Cell Biochem. 116, 696–703. https://doi.org/10.1002/jcb.25074.

Murphy, T.E., Rees, B.B., 2024. Diverse responses of hypoxia-inducible factor alpha mRNA abundance in fish exposed to low oxygen: the importance of reporting methods. Front. Physiol. 15, 2024. https://doi.org/10.3389/fphys.2024.1496226.

Nfon, E., Cousins, I.T., Järvinen, O., Mukherjee, A.B., Verta, M., Broman, D., 2009. Trophodynamics of mercury and other trace elements in a pelagic food chain from the Baltic Sea. Sci. Total Env. 407, 6267–6274. https://doi.org/10.1016/j.scitotenv.2009.08.032.

Nielsen, K.M., Venables, B., Roberts, A., 2016. Effects of dietary methylmercury on the dopaminergic system of adult fathead minnows and their offspring. Env. Toxicol. Chem. 36, 1077–1084. https://doi.org/10.1002/etc.3630.

Okeke, E.S., Nwankwo, C.E.I., Owonikoko, W.M., Emencheta, S.C., Ozochi, C.A., Nweze, E.J., Okeke, V.C., Nwuche, C.O., Enochoghene, A.E., 2024. Mercury's poisonous pulse: blazing a new path for aquatic conservation with eco-friendly mitigation strategies. Sci. Total Env. 957, 177719. https://doi.org/10.1016/j.scitotenv.2024.177719.

Olsvik, P.A., Williams, T.D., Tung, H.-S., Mirbahai, L., Sanden, M., Skjaerven, K.H., Ellingsen, S., 2014. Impacts of TCDD and MeHg on DNA methylation in zebrafish (*Danio rerio*) across two generations. Comp. Biochem. Physiol. C. Toxicol. Pharmacol. 165, 17–27. https://doi.org/10.1016/j.cbpc.2014.05.004.

Pacitti, D., Lawan, M.M., Sweetman, J., Martin, S.A.M., Feldmann, J., Secombes, C.J., 2016. Correction: selenium supplementation in fish: a combined chemical and biomolecular study to understand Sel-Plex assimilation and impact on selenoproteome expression in rainbow trout (*Oncorhynchus mykiss*). PLoS. One 11, e0144681. https://doi.org/10.1371/journal.pone.0144681.

Peterson, S.A., Ralston, N.V.C., Peck, D.V., Sickle, J.V., Robertson, J.D., Spate, V.L., Morris, J.S., 2009. How might selenium moderate the toxic effects of mercury in stream fish of the western U.S.? Env. Sci. Technol. 43 (10), 3919–3925. https://doi.org/10.1021/es803203g.

Piscopo, M., Notariale, R., Tortora, F., Lettieri, G., Palumbo, G., Manna, C., 2020. Novel insights into mercury effects on hemoglobin and membrane proteins in human erythrocytes. Molecules. 25, 3278. https://doi.org/10.3390/molecules25143278.

R Core Team, 2019. R: A Language and Environment for Statistical Computing. R Foundation for Statistical Computing, Vienna, Austria. https://www.R-project.org/.

Ralston, N.V.C., Ralston, C.R., Raymond, L.J., 2016. Selenium health benefit values: updated criteria for mercury risk assessments. Biol. Trace Elem. Res. 171, 262–269. https://doi.org/10.1007/s12011-015-0516-z.

Rasinger, J., Lundebye, A.-K., Penglase, S., Ellingsen, S., Amlund, H., 2017. Methylmercury induced neurotoxicity and the influence of selenium in the brains of adult zebrafish (*Danio rerio*). Int. J. Mol. Sci. 18, 725. https://doi.org/10.3390/ijms18040725.

Ravenna, L., Salvatori, L., Russo, M.A., 2016. HIF3α: the little we know. FEBS. J. 283, 993–1003. https://doi.org/10.1111/febs.13572.

Ribeiro, M., Zephyr, N., Silva, J.A.L., Danion, M., Guérin, T., Castanheira, I., Leufroy, A., Jitaru, P., 2022. Assessment of the mercury-selenium antagonism in rainbow trout fish. Chemosphere 286, 131749. https://doi.org/10.1016/j.chemosphere.2021.131749.

Robinson, M.D., McCarthy, D.J., Smyth, G.K., 2010. edgeR: a bioconductor package for differential expression analysis of digital gene expression data. Bioinformatics. 26, 139–140. https://doi.org/10.1093/bioinformatics/btp616.

Saito, T., Whatmore, P., Taylor, J.F., Fernandes, J.M.O., Adam, A.-C., Tocher, D.R., Espe, M., Skjærven, K.H., 2021. Micronutrient supplementation affects transcriptional and epigenetic regulation of lipid metabolism in a dose-dependent manner. Epigenetics. 16, 1217–1234. https://doi.org/10.1080/15592294.2020.1859867.

Saito, Y., 2021. Selenium transport mechanism via selenoprotein P-its physiological role and related diseases. Front. Nutr. 8, 2021. https://doi.org/10.3389/fnut.2021.685517.

Sandheinrich, M., Wiener, J., 2011. Methylmercury in freshwater fish. In: Bey, N., Meador, J.P. (Eds.), Environmental Contaminants in Biota. CRC Press, pp. 169–190. https://doi.org/10.1201/b10598-5.

Scheuhammer, A., Braune, B., Chan, H.M., Frouin, H., Krey, A., Letcher, R., Loseto, L., Noël, M., Ostertag, S., Ross, P., Wayland, M., 2015. Recent progress on our understanding of the biological effects of mercury in fish and wildlife in the Canadian Arctic. Sci. Total Env. 509–510, 91–103. https://doi.org/10.1016/j.scitotenv.2014.05.142.

Semenza, G.L., 2012. Hypoxia-inducible factors in physiology and medicine. Cell 148, 399–408. https://doi.org/10.1016/j.cell.2012.01.021.

Sies, H., Berndt, C., Jones, D.P., 2017. Oxidative stress. Annu. Rev. Biochem. 86, 715–748. https://doi.org/10.1146/annurev-biochem-061516-045037.

Stringari, J., Nunes, A.K.C., Franco, J.L., Bohrer, D., Garcia, S.C., Dafre, A.L., Milatovic, D., Souza, D.O., Rocha, J.B.T., Aschner, M., Farina, M., 2008. Prenatal methylmercury exposure hampers glutathione antioxidant system ontogenesis and causes long-lasting oxidative stress in the mouse brain. Toxicol. Appl. Pharmacol. 227, 147–154. https://doi.org/10.1016/j.taap.2007.10.010.

Taylor, C.T., Scholz, C.C., 2022. The effect of HIF on metabolism and immunity. Nat. Rev. Nephrol. 18, 573–587. https://doi.org/10.1038/s41581-022-00587-8.

Wang, H.-Q., Tuominen, L.K., Tsai, C.-J., 2011a. SLIM: a sliding linear model for estimating the proportion of true null hypotheses in datasets with dependence structures. Bioinformatics. 27, 225–231. https://doi.org/10.1093/bioinformatics/btq650.

Wang, F., Lemes, M., Khan, M.A.K., 2011b. Metallomics of mercury: role of thiol- and selenol-containing biomolecules. In: Liu, G., Cai, Y., O'Driscoll, N. (Eds.), Environmental Chemistry and Toxicology of Mercury. Wiley. https://doi.org/10.1002/9781118146644.ch16.

Wang, H., Chen, B., He, M., Yu, X., Hu, B., 2017. Selenocystine against methyl mercury cytotoxicity in HepG2 cells. Sci. Rep. 7, 147. https://doi.org/10.1038/s41598-017-00231-7.

Wei, Y., Ni, L., Pan, J., Li, X., Xu, B., Deng, Y., Yang, T., Liu, W., 2021. The roles of oxidative stress in regulating autophagy in methylmercury-induced neurotoxicity. Neuroscience 469, 175–190. https://doi.org/10.1016/j.neuroscience.2021.06.026.

Weinhouse, C., Perez, L., Ryde, I., Goodrich, J.M., Miranda, J.J., Hsu-Kim, H., Murphy, S. K., Meyer, J.N., Pan, W.K., 2022. Epigenetic biomarkers of autoimmune risk and protective antioxidant signaling in methylmercury-exposed adults. bioRxiv https://doi.org/10.1101/2022.07.05.498896.

West, A.K., Hidalgo, J., Eddins, D., Levin, E.D., Aschner, M., 2008. Metallothionein in the central nervous system: roles in protection, regeneration and cognition. Neurotoxicology. 29, 489–503. https://doi.org/10.1016/j.neuro.2007.12.006.

Wiener, J.G., Krabbenhoft, D., Heinz, G.H., Scheuhammer, A.M., 2002. Ecotoxicology of mercury. In: Hoffman, D.J., Rattner, B.A., Burton Jr., G.A., Cairns Jr., J. (Eds.), Handbook of Ecotoxicology. CRC Press, pp. 409–463. https://doi.org/10.1201/9781420032505.ch16.

Wischhusen, P., Saito, T., Heraud, C., Kaushik, S.J., Fauconneau, B., Prabhu, P.A.J., Fontagné-Dicharry, S., Skjærven, K.H., 2020. Parental selenium nutrition affects the one-carbon metabolism and the hepatic DNA methylation pattern of rainbow trout (*Oncorhynchus mykiss*) in the progeny. Life 10, 121. https://doi.org/10.3390/life10080121.

Yadetie, F., Karlsen, O.A., Lanzén, A., Berg, K., Olsvik, P., Hogstrand, C., Goksøyr, A., 2013. Global transcriptome analysis of Atlantic cod (*Gadus morhua*) liver after in vivo methylmercury exposure suggests effects on energy metabolism pathways. Aquat. Toxicol. 126, 314–325. https://doi.org/10.1016/j.aquatox.2012.09.013.

Yu, G., Wang, L.-G., Han, Y., He, Q.-Y., 2012. clusterProfiler: an R package for comparing biological themes among gene clusters. OMICS. 16, 284–287. https://doi.org/10.1089/omi.2011.0118.

Zhang, P., Yao, Q., Lu, L., Li, Y., Chen, P.-J., Duan, C., 2014. Hypoxia-inducible factor 3 is an oxygen-dependent transcription activator and regulates a distinct transcriptional response to hypoxia. Cell Rep. 6, 1110–1121. https://doi.org/10.1016/j.celrep.2014.02.011.